Neutron powder diffraction study of hydrogarnet to 9.0 GPa

GEORGE A. LAGER[1] AND ROBERT B. VON DREELE[2]

[1]Department of Geography and Geosciences, University of Louisville, Louisville, Kentucky 40292, U.S.A.
[2]LANSCE, Los Alamos National Laboratory, Los Alamos, New Mexico 87545, U.S.A.

ABSTRACT

The crystal structure of synthetic, deuterated katoite [$Ca_3Al_2(O_4D_4)_3$] has been refined at 0.0001, 0.78, 3.6, 6.1, 7.9, and 9.0 GPa using the opposed-anvil Paris-Edinburgh cell and the POLARIS powder diffractometer at the U.K. pulsed spallation source, ISIS. A constrained Birch-Murnaghan fit to the unit-cell volume yields $K_0 = 52(1)$ GPa for $K_0' \equiv$ 4.0. The lower bulk modulus of katoite relative to anhydrous Ca-bearing garnets ($K_0 =$ 159–179 GPa) is due to the greater compressibility of the Ca dodecahedron and O_4D_4 tetrahedron. At high pressure, corner-sharing tetrahedra and octahedra undergo a rigid-body rotation, which causes a shift in the O position. This rotation, coupled with the large compression of the two tetrahedral edges shared with the dodecahedron, changes the relative lengths of the Ca-O bonds at high pressure, such that Ca2-O < Ca1-O for $P > 6$ GPa. With increasing pressure, the O-D$\cdots$O angles widen slightly, as the O-D vector rotates toward the tetrahedral face. Both O-D and O$\cdots$D bond lengths decrease as a function of pressure, which was unexpected in view of the results of recent high-pressure studies. Comparison of crystallographic and spectroscopic data collected at high pressure for hydrogarnets suggests that empirical relationships derived for hydrogen-bond systems at ambient conditions, where a relaxed, equilibrium state is attained, may not always apply to O-D$\cdots$O hydrogen bonds under compression.

INTRODUCTION

The substitution $O_4H_4 = SiO_4$ is an effective mechanism for incorporating H into the crystal structures of garnet. This observation, coupled with the fact that garnet is stable at high temperature and pressure, suggests that hydrogarnets are possible storage sites for H in the Earth's mantle (Aines and Rossman 1984a, 1984b). However, until recently, very little was known about the effect of structurally bound OH on the physical properties of garnet. O'Neill et al. (1988) measured the elastic properties of a solid-solution member ($Gr_{60}Ka_{40}$) of the series [$Ca_3Al_2(SiO_4)_3$ (grossular)–$Ca_3Al_2(O_4H_4)_3$ (katoite)] at ambient conditions by Brillouin spectroscopy and observed that the $O_4H_4 = SiO_4$ substitution reduces both the shear and bulk moduli by 40% relative to grossular. Olijnyk et al. (1991) determined the unit-cell volumes of both grossular and katoite from energy-dispersive X-ray diffraction methods at pressures to 18 and 42 GPa, respectively. The lower bulk modulus of katoite relative to grossular [66(4) vs. 168(25)] was attributed primarily to the lower bulk modulus of the O_4H_4 tetrahedron. Knittle et al. (1992) collected high-pressure (16 GPa) Raman and infrared (IR) spectra in the O-H–stretching region for a synthetic hibschite ($Gr_{50}Ka_{50}$) and concluded that (1) the lower bulk modulus relative to grossular reflected the high compressibility of the O_4H_4 tetrahedron, and (2) the negative pressure shift of IR and Raman bands was consis-

tent with an increase in the strength of the hydrogen bond and a lengthening of the O-H bond at high pressure. The latter argument has also been used to explain negative pressure shifts of IR bands in $Mg(OH)_2$ (Kruger et al. 1989), chondrodite (Williams 1992), and kaolinite and aluminous serpentine (Velde and Martinez 1981).

A key element missing from these studies is a crystal-structure description of the compression mechanism in hydrogarnet. To date, structure refinements at high pressure have been limited to single-crystal X-ray diffraction studies of anhydrous garnets: pyrope (Py_{100}) and grossular (Gr_{100}) (Hazen and Finger 1978), and pyrope ($Py_{67}Al_{19}Gr_{10}An_3Sp_1$) and andradite ($An_{100}$) (Hazen and Finger 1989). The latter study, in which a new data-collection procedure was employed, provides the most precise information to date on the compressibility of silicate garnets. The mechanism of compression in andradite involves a cooperative rotation of the Al octahedra and SiO_4 tetrahedra, which share corners to form a three-dimensional framework. With increasing pressure, the net effect of these rotations is the collapse of the framework about the large dodecahedral (Ca) cavity. The observation that the O_4H_4 tetrahedron is more compressible than the SiO_4 tetrahedron suggests that H may play an important role in the compression of hydrogarnet. The development of stronger hydrogen bonds at high pressure could be responsible, in part, for the high compressibility of the O_4H_4 tetrahedron and the structural stability of the O_4H_4

group at mantle pressures. Both Raman and IR spectra for hibschite suggest that increased pressure enhances the weak hydrogen bonding in hydrogarnet. However, spectroscopic studies are presently limited by the lack of quantitative information on H(D)-atom positions as a function of pressure. Because H is a weak X-ray scatterer, the effect of pressure on the H position must be determined by neutron diffraction methods.

With the recent development of the Paris-Edinburgh cell (Besson et al. 1992) at pulsed spallation sources, neutron powder data can be routinely collected to pressures of ~10 GPa using tungsten carbide (WC) anvils (see, for example, Parise et al. 1994). In the present study, the crystal structure of katoite was refined at 0.0001, 0.78, 3.6, 6.1, 7.9, and 9.0 GPa to determine the effect of O_4D_4 = SiO_4 substitution on garnet compression and to quantify the pressure dependence of the O-D···O hydrogen-bond geometry. This study represents the first neutron diffraction refinement of a moderately complex mineral structure ($V = $ ~2000 Å^3, $Z = 8$) at pressures in excess of ~3 GPa.

EXPERIMENTAL METHODS

A polycrystalline sample of katoite was synthesized at 473 K and 200 bars following the procedure outlined by Lager et al. (1987). X-ray diffraction and IR reflectance spectroscopy were used to check sample purity and crystallinity. A 130 mg sample of deuterated katoite was mixed with 36 mg of NaCl, which was used as an internal pressure calibrant. Sufficient fluorinert FC-70 (3M Company) was then added to this mixture to form a thick paste, which was loaded into the Paris-Edinburgh high-pressure cell (Besson et al. 1992). The sample was contained by null-scattering Ti-Zr alloy gaskets located between WC anvils. The sample shape was spheroidal with a total volume of 100 mm^3. Oil pressure in the ram was raised using a hand pump.

Time-of-flight neutron powder diffraction data were collected at 0.0001, 0.78, 3.6, 6.1, 7.9, and 9.0 GPa in the 90° detector banks of the POLARIS diffractometer at the U.K. pulsed spallation source, ISIS. The POLARIS instrument is a high-intensity, medium-resolution ($\Delta d/d$ = ~7 × 10^{-3} for $2\theta = 90°$) diffractometer with a flight path of 12.0 m. It is situated on beamline S1 at ISIS and receives a polychromatic "white" beam of neutrons from a 295 K H$_2$O moderator (Smith and Hull 1994). Data-collection times on the spallation source ranged from 9.31 h (1340 μA·h) to 14.15 h (2125 μA·h) for the nonambient experiments. Because of limited neutron beam time, data were collected at ambient pressure in the pressure cell for only 4 h (633 μA·h). A 10% drop in pump pressure was noted during data collection at 9.0 GPa. The effect of this pressure drop on the 9.0 GPa data set is unknown; however, the D-atom position at 9.0 GPa appears to be anomalous.

The data were corrected for absorption by the anvils and normalized to the incident spectrum using a local routine. Rietveld (1969) profile analysis for multiple-phase samples (katoite, NaCl, and WC), as coded in the General Structure Analysis System (GSAS) (Larson and Von Dreele 1994), was used for the structure refinements. Although the WC anvils were shielded with cadmium foil, Bragg scattering from the anvils was observed in all profiles. Starting parameters for the katoite refinement were taken from Lager et al. (1987). The refinement model at each pressure included ~1200 allowed garnet reflections in the d range ~0.41–2.75 Å. The unit-cell parameter for katoite and NaCl refined from data collected at ambient pressure in the cell was significantly less than previously reported, probably because of a slight displacement of the sample position. To correct for this effect, the unit-cell parameter for both phases was fixed at known values, and the C diffractometer constant was refined. In all subsequent refinements at higher pressure, the value of C was fixed at the ambient-pressure value and the unit-cell parameters were varied. An isotropic microstrain parameter was also refined at higher pressures to characterize the pressure-induced broadening. The strain, calculated from the γ coefficient of the TOF profile function (function 3; Larson and Von Dreele 1994), varied from 0.13% at 0.78 GPa to 2.0% at 9.0 GPa. A total of 27 variables were refined at ambient pressure; 29 parameters were varied in refinements at nonambient pressures. The background was modeled by a power function in Q (function 4; Larson and Von Dreele 1994). On the basis of refinement of the D-site occupancy, the sample was ~93% deuterated. The pressures were determined from the refined unit-cell parameter and the equation of state for NaCl (Decker 1971). Discrepancy indices and refined unit-cell and atomic parameters are given in Table 1. Final refinement profiles at 0.0001 and 7.9 GPa are compared in Figure 1. The variation in selected interatomic distances and angles as a function of pressure is presented in Table 2. Table 2 also shows a comparison between the ambient-pressure refinement of this study and that reported by Lager et al. (1987), who obtained time-of-flight neutron powder data at 300 K and 1 bar from a katoite sample packed in a vanadium can. Although significant differences exist between these refinements, particularly in the case of distances and angles involving D, the data collected in the present study are generally more consistent with results obtained from the high-pressure refinements. Because we are primarily interested in relative changes as a function of pressure, the results from this study have been used as the ambient-pressure point in the plots that follow.

→

FIGURE 1. Comparison of final refinement profiles at 0.0001 (**a**) and 7.9 GPa (**b**). Plus signs represent observed data. Solid line is best-fit profile. Tick marks below the profile indicate the positions of all allowed reflections for each of the three phases: katoite, NaCl, and WC from bottom to top. Background was fitted as part of the refinement but was subtracted before plotting.
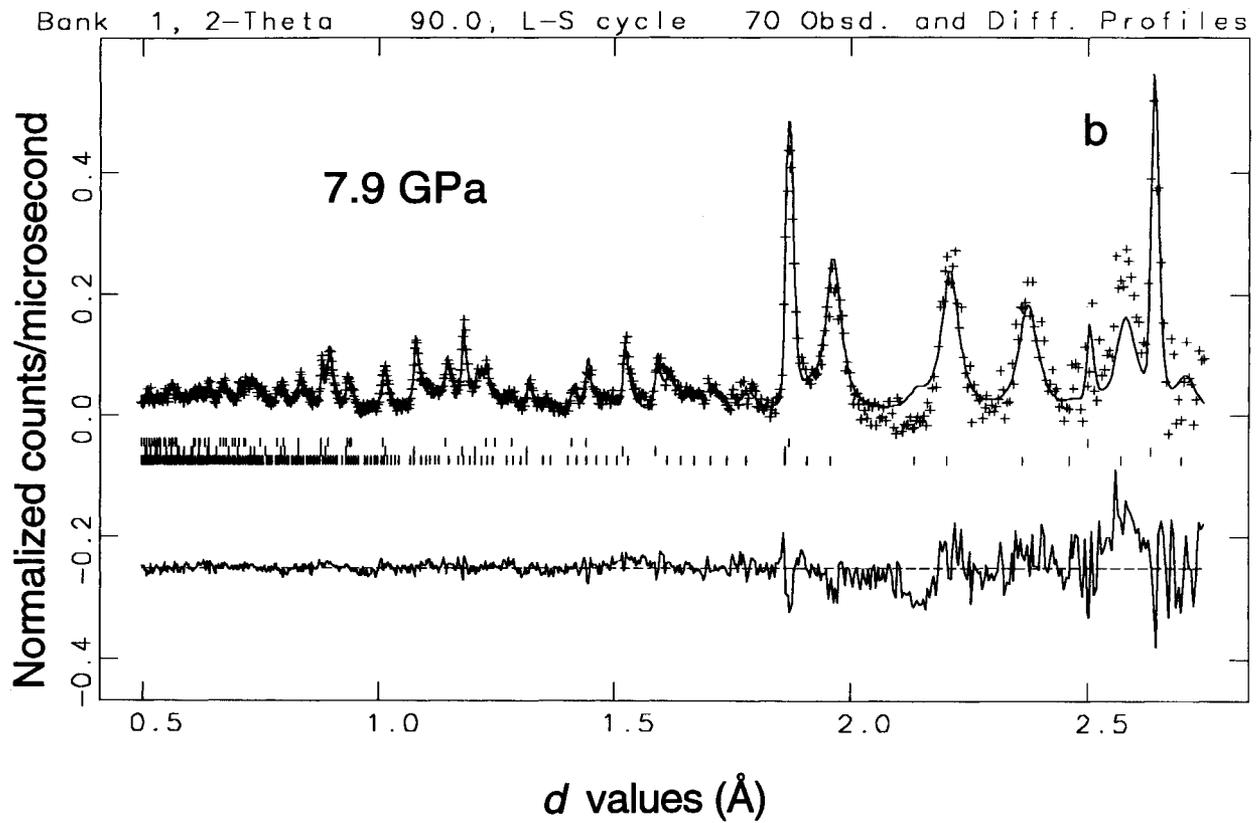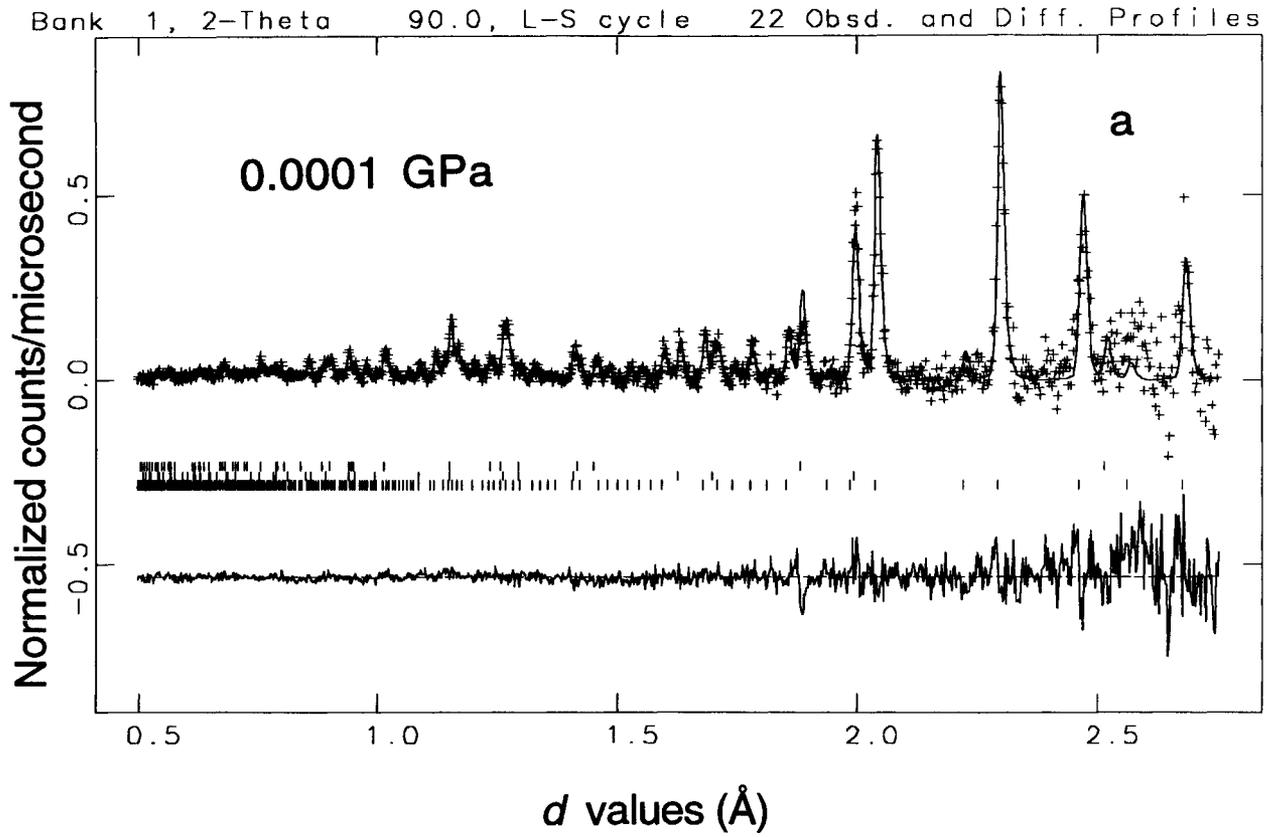
TABLE 1. Discrepancy indices and refined unit-cell and atomic parameters

P (GPa)	0.0001*	0.78	3.6	6.1	7.9	9.0
R_{wp} (%)**	3.49	2.38	2.28	2.22	2.18	2.17
R_p (%)	6.03	4.06	4.00	3.74	3.64	3.69
χ^2	1.82	2.29	1.89	2.13	2.45	2.76
a (Å)	12.5695(11)	12.5130(6)	12.320(2)	12.163(2)	12.077(4)	12.024(4)
V (Å³)	1985.9(3)	1959.2(2)	1870.2(2)	1799.2(5)	1761.3(9)	1738.3(10)
U_{iso} (Ca)†	0.6(2)	0.7(2)	0.3(2)	0.01(2)	0.01(2)	0.05(3)
U_{iso} (Al)	1.6(5)	0.06(2)	0.9(4)	0.6(4)	2.0(8)	3.1(1)
O						
x	0.0278(5)	0.0282(4)	0.0301(5)	0.0306(5)	0.0306(8)	0.0297(10)
y	0.0525(5)	0.0525(4)	0.0533(4)	0.0550(5)	0.0561(8)	0.0559(9)
z	0.6392(5)	0.6392(3)	0.6398(4)	0.6405(4)	0.6401(6)	0.6404(8)
U_{iso}	1.2(2)	0.9(1)	0.8(1)	0.4(1)	0.4(2)	0.5(2)
D						
x	0.1517(10)	0.1531(9)	0.1533(12)	0.1550(14)	0.158(2)	0.163(3)
y	0.0919(10)	0.0923(9)	0.0873(12)	0.0828(14)	0.082(2)	0.087(3)
z	0.7939(10)	0.7934(8)	0.7946(10)	0.7927(11)	0.794(2)	0.795(2)
U_{iso}	3.1(5)	2.9(4)	3.7(5)	4.2(6)	2.9(8)	2.6(9)

Note: Space group $Ia\bar{3}d$ with Ca at site 24c (⅛, 0, ¼), Al at site 16a (0, 0, 0), Si at site 24d (⅜, 0, ¼). Numbers in parentheses are estimated standard deviations and refer to the last decimal place cited.
 * Data collected in pressure cell.
 ** Refer to Larson and Von Dreele (1994) for definition of discrepancy indices.
 † Isotropic displacement factor in units of squared angstroms times 100.

RESULTS AND DISCUSSION

The general formula of hydrogarnet can be represented as $^{[8]}X^{[6]}Y(^{[4]}SiO_4)_{3-x}(O_4H_4)_x$ where the superscripts in brackets refer to the O coordination of three types of cation sites in the structure. The O coordination of the X site can be defined by a triangular dodecahedron (distorted cube) that shares two edges with tetrahedra, four with octahedra (Y site), and four with other dodecahedra. The dodecahedral cavities are located within a framework composed of corner-sharing octahedra and tetrahedra (Novak and Gibbs 1971). The hydrogarnet structure is uniquely defined by the fractional coordinates (x,y,z) of the O and H atoms and the unit-cell parameter. The cations occupy special positions that are fixed by symmetry (refer to footnote in Table 1). When the tetrahedron is not occupied by Si, each O atom surrounding the vacancy is covalently bonded to an H atom (Fig. 2).
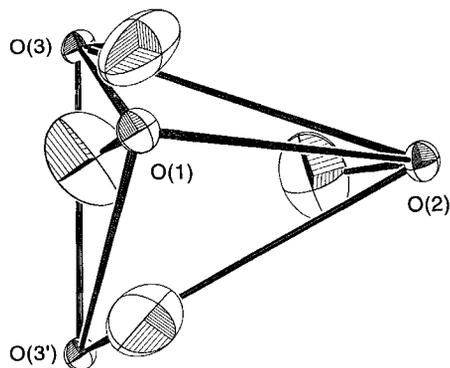
FIGURE 2. Atomic environment of the $\bar{4}$ site in katoite, showing the O tetrahedron with associated D atoms (from Lager et al. 1987).

Occupied and unoccupied sites are distributed randomly in the structure, preserving the space group symmetry ($Ia\bar{3}d$).

The O-H vector in katoite lies slightly outside the tetrahedron and is nearly parallel to the O-O-O bisector in the tetrahedral face, e.g., face O3-O1-O3' in Figure 2. As a result, two O atoms in each face are located approximately equidistant from H and are involved in a weak, bifurcated hydrogen bond (Harmon et al. 1982). $O\cdots D$ distances and associated O-D$\cdots$O angles are 2.567(2) and 2.497(2) Å and 132.1(1) and 140.1(1)°, respectively (Lager et al. 1987). It should be noted that the existence of a hydrogen bond in katoite is difficult to substantiate because the IR frequency of the O-H–stretching band ($\sim$3662 cm^{-1}) is significantly greater than the value (3556 cm^{-1}) experimentally determined for the stretching fundamental in free, gaseous OH$^-$ (Owrutsky et al. 1985). Lutz (1995) suggested that hydrogen bonding must be considered if the observed O-H frequency is 10 or more inverse centimeters less than the value calculated from the relationship between the mean M-O distance and the O-H–stretching frequency (Lutz 1995, Fig. 6). On the basis of the calculated frequency (3701 cm^{-1}) for Al-O = 1.916 Å in katoite, one would predict a weak O-H$\cdots$O hydrogen bond.

The large displacement amplitude perpendicular to the O-H bond (Fig. 2) and the short O-H bond length [0.906(2) vs. 0.964 Å in free, gaseous OH$^-$] suggest possible disorder of the D atoms (Lager et al. 1987). In view of the recent studies of both deuterated and hydrogenated brucite [Mg(OH)$_2$], in which H(D) was found to disorder with increasing pressure (Parise et al. 1994; Catti et al. 1995), anisotropic displacement factors for D in katoite were examined at various pressures for any unusual increase in anisotropy. No evidence was found to support a pressure-dependent positional disorder of D.

TABLE 2. Selected interatomic distances (Å) and angles (°)

P (GPa)	0.0001*	0.0001**	0.78	3.6	6.1	7.9	9.0
			Tetrahedron				
d-O × 4	1.950(2)	1.967(6)	1.955(5)	1.908(5)	1.881(6)	1.876(10)	1.871(13)
O1-O2 × 2	3.058(2)	3.082(12)	3.067(9)	3.016(9)	2.981(1)	2.980(15)	2.96(2)
O1-O3 × 4	3.245(2)	3.275(12)	3.252(9)	3.164(11)	3.118(11)	3.11(2)	3.10(2)
Mean O-O	3.183	3.211	3.190	3.115	3.072	3.067	3.053
			O_4D_4 **tetrahedral environment**				
O-D × 4	0.906(2)	0.925(12)	0.898(10)	0.873(13)	0.862(15)	0.83(2)	0.75(3)
O···D	2.497(2)	2.536(14)	2.538(14)	2.44(2)	2.40(2)	2.41(3)	2.48(4)
	2.567(2)	2.54(2)	2.532(14)	2.47(2)	2.41(2)	2.43(3)	2.49(4)
D-D	1.956(2)	1.93(2)	1.94(2)	1.85(3)	1.76(3)	1.78(4)	1.91(6)
O-D···O	132.1(1)	136.8(10)	137.6(4)	136.5(5)	139.1(12)	139(2)	141(2)
	140.1(1)	137.2(11)	137.0(10)	140.4(5)	141.1(12)	142.9(13)	142(3)
			Other distances involving D				
d-D	1.343(2)	1.323(13)	1.324(12)	1.26(2)	1.19(2)	1.19(3)	1.27(4)
Al-D	2.425(2)	2.404(13)	2.378(12)	2.40(2)	2.40(2)	2.37(3)	2.28(3)
Ca-D	3.094(2)	3.085(12)	3.056(10)	2.986(13)	2.91(2)	2.85(2)	2.81(3)
Ca-D	2.851(2)	2.901(13)	2.885(11)	2.835(14)	2.82(2)	2.78(2)	2.71(3)
			Octahedron				
Al-O × 6	1.916(2)	1.903(6)	1.895(14)	1.881(5)	1.872(5)	1.860(8)	1.852(10)
O1-O4 × 6	2.604(2)	2.571(11)	2.566(8)	2.565(10)	2.547(11)	2.525(7)	2.51(2)
O1-O5 × 6	2.811(2)	2.805(11)	2.789(8)	2.752(9)	2.743(9)	2.731(14)	2.73(2)
Mean O-O	2.707	2.688	2.678	2.659	2.645	2.628	2.62
			Dodecahedron				
Ca1-O4 × 4	2.464(2)	2.462(6)	2.455(4)	2.435(5)	2.409(5)	2.398(8)	2.377(9)
Ca2-O4 × 4	2.521(2)	2.513(7)	2.503(5)	2.458(6)	2.408(6)	2.377(10)	2.369(11)
Mean	2.493	2.488	2.479	2.447	2.409	2.388	2.373

Note: d is the Wyckoff notation for the position with point symmetry $\bar{4}$ in space group $Ia\bar{3}d$ (occupied by Si in silicate garnets). Numbers in parentheses are estimated standard deviations and refer to the last decimal place cited.
* Data collected at ambient pressure from sample in vanadium can (Lager et al. 1987).
** Data collected at ambient pressure from sample in pressure cell.

A second-order Birch-Murnaghan fit to the unit-cell volumes in Table 1 yields a bulk modulus $K_0 = 52(1)$ GPa [0.0004(4) Å/GPa]. Brucite, like katoite, exhibits a weak hydrogen-bond interaction at ambient pressure, i.e., O···H bond lengths in both structures are ~2.5 Å. At higher pressures, hydrogen bonding between octahedral pressure (5.7–42.3 GPa) was calculated from the positions of four reflections (321, 400, 420, and 521) fit by pure Gaussian profiles. With the assumption that the pressure calibration is comparable in both studies, the K_0 value determined in the present study should be more precise because the whole profile was fit by least-squares methods. However, systematic differences between neutron and X-ray diffraction results are not unusual and, in this case, could be due to a variety of factors, such as H-D isotope effects, deviatoric stress, sample placement, or energy calibration.

The mechanism of compression in katoite is similar, in some respects, to that observed in andradite (Hazen and Finger 1989). With increasing pressure, corner-sharing tetrahedra and octahedra undergo a rigid-body rotation (Fig. 3) as the garnet framework collapses about the large dodecahedral (Ca) cavity. As a result of this rotation, the O4 atom shifts toward Ca, shortening the long Ca-O distance (Ca2-O) (Fig. 4).

As proposed by Olijnyk et al. (1991) and Knittle et al. (1992), the O_4H_4 tetrahedron is more compressible than the SiO_4 tetrahedron. The rate of compression of the shared (O1-O2) and unshared (O1-O3) tetrahedral edges

in katoite is significantly greater (0.014 and 0.019 Å/GPa) than that observed for the corresponding edges in andradite (0.003 and 0.006 Å/GPa) (Hazen and Finger 1989). The greater compressibility of the O_4H_4 tetrahedron has a pronounced effect on the long Ca-O bond, which has a large vector component in the direction of the two tetrahedral edges shared with the dodecahedron (Fig. 4). The rigid-body rotation noted above, coupled with the large compression of these two edges, causes the long Ca-O bond to compress at a significantly greater rate than the short bond in the dodecahedron, such that Ca2-O < Ca1-O for pressures >6 GPa (Fig. 5). This effect has not been observed in anhydrous garnets at high pressure because the SiO_4 tetrahedron is relatively incompressible. It should be noted that the lower bulk modulus of katoite relative to anhydrous Ca-bearing garnets ($K_0 = 159$–179 GPa; Olijnyk et al. 1991) is due to the greater compressibility of both the tetrahedron and dodecahedron. The bulk modulus for both polyhedra is approximately equal to the bulk modulus of the sample. For comparison, the bulk moduli of corresponding polyhedra in andradite are 200 and 160 GPa, respectively (Hazen and Finger 1989).

The pressure dependence of selected distances and angles involving D is summarized in Figures 6 and 7. Although the estimated standard deviations in some cases are large, several important trends can be recognized: (1) Both the O-D and O···D bond lengths decrease as a function of pressure. The change in O-D is greater than that in O···D by a factor of four if the 9.0 GPa measurement
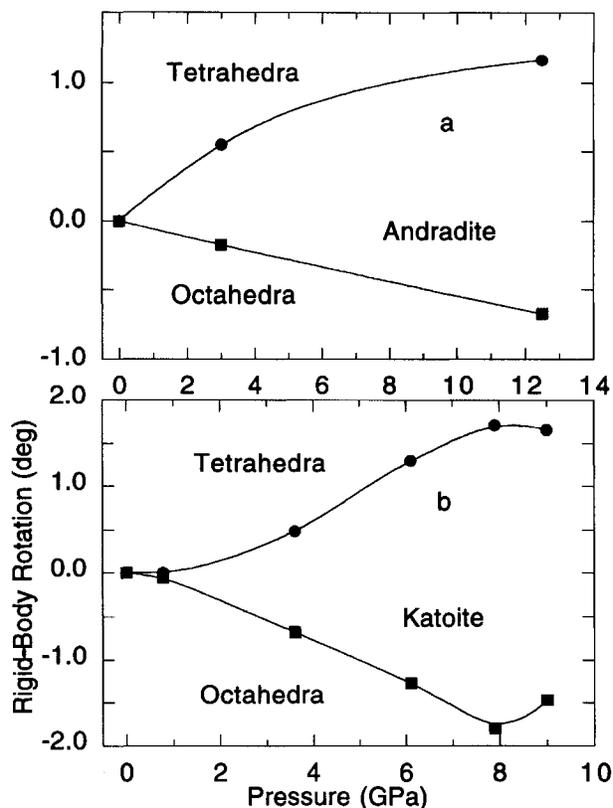
FIGURE 3. Relative rigid-body rotations of tetrahedra and octahedra in andradite (a) and katoite (b) as a function of pressure. Rotations were calculated with the computer program POLYSTRAIN (Lager 1978).

is included. Even without this data point, which appears to be anomalous, the change in O-D (10%) is twice as great as that in O···D (5%). At ambient pressure, shorter O···H distances imply a decrease in the O-H bond strength, which may result in a lengthening of the O-H bond. (2) The O-D···O angles widen slightly as a function of pressure. (3) The short D-D distance [1.93(2) Å] between adjacent OH groups (Fig. 2) decreases at high pressure [1.78(4) Å at 7.9 GPa]. In inorganic structures, H atoms are predicted to be at least 2.0 Å apart, on the basis of the van der Waals radius for H (1.0 Å) (Baur 1972).

It is interesting to compare O-D bond-length variation in katoite with that in ice VIII (Nelmes et al. 1993; Besson et al. 1994) and Mg(OH)$_2$ brucite (Parise et al. 1994; Catti et al. 1995). In ice VIII, which is characterized by moderately strong hydrogen bonding, a small increase in O-D bond length has been observed at pressures to 10 GPa [0.0004(4) Å/GPa]. Brucite, like katoite, exhibits a weak hydrogen-bond interaction at ambient pressure, i.e., O···H bond lengths in both structures are ~2.5 Å. At higher pressures, hydrogen bonding between octahedral layers in brucite becomes stronger as the interlayer O··· D distance decreases to slightly <2 Å at 9.3 GPa (Parise
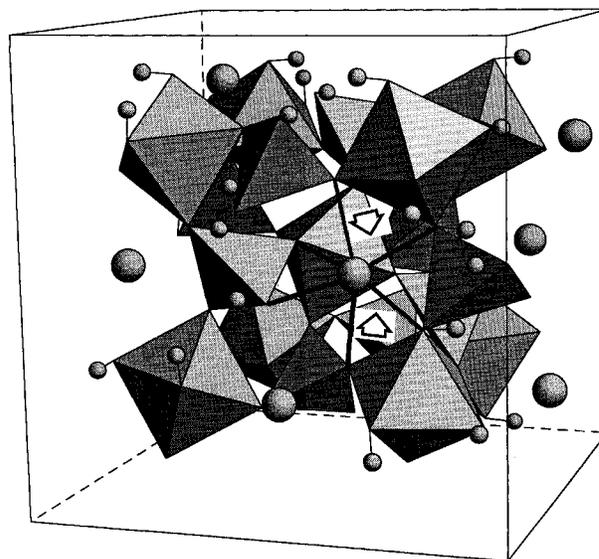
FIGURE 4. Portion of the katoite unit cell, illustrating the framework of corner-sharing tetrahedra and octahedra and the orientation of the O-H vectors. The large solid sphere in the center of the drawing represents Ca, which is coordinated to eight O atoms located at the corners of a distorted cube (dodecahedron). The four short Ca-O bonds are opposite the two edges shared between the dodecahedron and tetrahedron. For clarity, only two of the four long bonds are shown. The O4 atom is displaced in the direction of Ca (arrows), as octahedra and tetrahedra undergo rigid-body rotations at high pressure.

et al. 1994). The O-D bond length increases from 0.95(1) to 1.021(9) Å in the pressure range 0.4–9.3 GPa. The O-H bond length in hydrogenated Mg(OH)$_2$ shows a slight decrease in length from 0.919(3) to 0.902(7) Å (at 10.9 GPa) if the disordered structure is assumed at high pressure (Catti et al. 1995). In contrast to the above structures, katoite exhibits only weak hydrogen bonding at high pressure (Table 2), which could explain the unexpected behavior of the O-D bond.
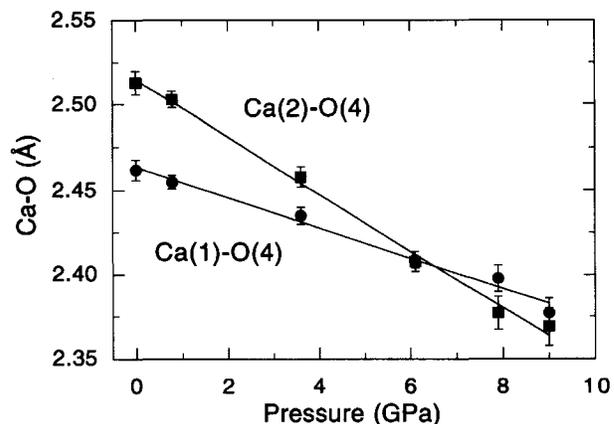
FIGURE 5. Variation of two unique Ca-O distances in the dodecahedron as a function of pressure.
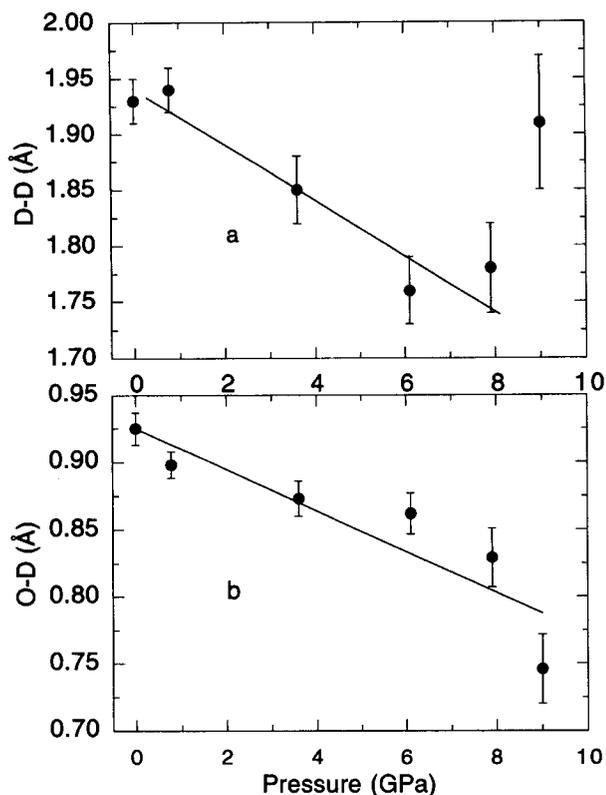
FIGURE 6. Variation of D-D (a) and O-D (b) distances as a function of pressure. The trends defined for both distances were fitted visually and exclude the distance at 9.0 GPa.

FIGURE 7. Variation of O-D···O angles (a) and O···D distances (b) as a function of pressure. The trend defined for O··· D distances was fit visually and excludes the distance at 9.0 GPa. The trends shown for the angles represent least-squares fits to the data.

The D atom in katoite most likely adopts a position that minimizes increased cation-cation repulsion caused by the shortening of Ca-D, Al-D, and, in particular, D-D distances at high pressure (Table 2). This idea is consistent with both the wider O-D···O angles, which result from rotation of the O-D vector toward the tetrahedral face (Fig. 2), and the shorter O-D bond length. The shorter O···D bond distances primarily reflect compression of O···O tetrahedral edges.

Although high-pressure IR spectra of katoite have not been reported, some inferences with respect to the pressure dependence of the OH band can be made on the basis of the work by Knittle et al. (1992). The two OH bands in the IR spectra of hibschite (3670 and 3608 cm^{-1}) can be interpreted as a linear superposition of two spectral components that originate from two OH environments (Lager et al. 1989). The weaker band (3608 cm^{-1}), which is not present in the katoite spectra at ambient pressure, may originate from O$_4$H$_4$ groups located adjacent to SiO$_4$ groups in solid-solution members of the grossular-katoite series (Rossman and Aines 1991). The stronger IR band (3670 cm^{-1}) is related to vibrations of OH groups in O$_4$H$_4$ tetrahedra, and, therefore, its behavior at high pressure should be similar in hibschite and katoite. The pressure dependence of the frequency of this band in hibschite is $-0.9(1)$ cm^{-1} GPa^{-1}, which is too

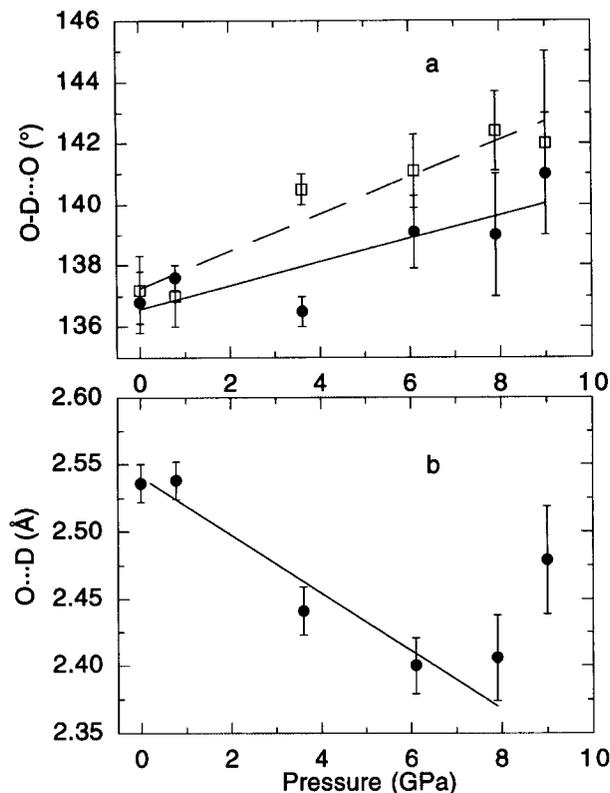small to explain the 5% shortening in the O···O distance in katoite over 9 GPa (Nakamoto et al. 1955). The frequency of OH bands in structures with weak hydrogen bonds should be most sensitive to changes in O-H bond length (Kubicki et al. 1993). On the basis of the empirical relationship between O-H bond length (r_{OH}) and O-H-stretching frequency (ν_{OH}) at ambient pressure (Novak 1974), the decrease in O-H bond length observed in this study would be expected to produce a large positive frequency shift with pressure ($\Delta\nu_{OH}/\Delta r_{OH} \approx 11000$ cm^{-1}). The small negative pressure shift of the 3670 cm^{-1} band in hibschite and the lack of an inverse correlation between O-D and O···D bond lengths in katoite suggest that relationships derived from hydrogen-bonded systems at ambient pressures, where a relaxed, equilibrium state is attained, may not always apply to O-D···O hydrogen bonds under compression (Nelmes et al. 1993). In particular, the geometry of the O-D···O bond as a function of pressure in katoite may be governed by other factors, such as D-D repulsion between adjacent OD groups. It is interesting to note that both O-H-stretching bands in the Raman spectra of hibschite also show negative pressure shifts but of a magnitude consistent with the observed compression of the mean O···O distance in

the tetrahedron. Knittle et al. (1992) attributed the larger negative shifts in the Raman spectra to intrinsic differences between the two types of spectroscopies; i.e., out-of-phase H motions for IR vs. in-phase motions for Raman. Further comparisons of crystallographic and spectroscopic data collected at high pressure for both hydrogenated and deuterated hydrogarnet are needed to interpret the significance of the pressure shifts in the O-H–stretching frequencies.

REFERENCES CITED

Aines, R.D., and Rossman, G.R. (1984a) Water content of mantle garnets. Geology, 12, 720–723.
——— (1984b) The hydrous component in garnets: Pyralspites. American Mineralogist, 69, 1116–1126.
Baur, W.H. (1972) Prediction of hydrogen bonds and hydrogen atom positions in crystalline solids. Acta Crystallographica, B28, 1456–1465.
Besson, J.M., Nelmes, R.J., Hamel, G., Loveday, J.S., Weill, G., and Hull, S. (1992) Neutron powder diffraction above 10 GPa. Physica B, 180 and 181, 907–910.
Besson, J.M., Pruzan, P., Klotz, S., Hamel, G., Silvi, B., Nelmes, R.J., Loveday, J.S., and Wilson, R.M. (1994) Variation of intertomic distances in ice VIII to 10 GPa. Physical Review B, 49, 12540–12550.
Catti, M., Ferraris, G., Hull, S., and Pavese, A. (1995) Static compression and H disorder in brucite, $Mg(OH)_2$, to 11 GPa: A powder neutron diffraction study. Physics and Chemistry of Minerals, 22, 200–206.
Decker, D.L. (1971) High-pressure equation of state for NaCl, KCl and CsCl. Journal of Applied Physics, 42, 3239–3244.
Harmon, K.M., Gabriele, J.M., and Nuttall, A.S. (1982) Hydrogen bonding in the tetrahedral $O_4H_4^{4-}$-cluster in hydrogrossular. Journal of Molecular Structure, 82, 213–219.
Hazen, R.M., and Finger, L.W. (1978) Crystal structures and compressibilities of pyrope and grossular to 60 kbar. American Mineralogist, 63, 297–303.
——— (1989) High-pressure crystal chemistry of andradite and pyrope: Revised procedures for high-pressure diffraction experiments. American Mineralogist, 74, 352–359.
Knittle, E., Hathorne, A., Davis, M., and Williams, Q. (1992) A spectroscopic study of the high-pressure behavior of the O_4H_4 substitution in garnet. In Y. Syono and M.H. Manghnani, Eds., High-pressure research: Application to earth and planetary sciences, Geophysical Monograph 67, American Geophysical Union, 297–304.
Kruger, M.B., Williams, Q., and Jeanloz, R. (1989) Vibrational spectra of $Mg(OH)_2$ and $Ca(OH)_2$ under pressure. Journal of Chemical Physics, 91, 5910–5915.

Kubicki, J.D., Sykes, D., and Rossman, G.R. (1993) Calculated trends of OH infrared stretching vibrations with composition and structure in aluminosilicate molecules. Physics and Chemistry of Minerals, 30, 425–432.
Lager, G.A. (1978) A novel technique for characterizing the thermal expansion in minerals. Physics and Chemistry of Minerals, 3, 237–249.
Lager, G.A., Armbruster, T., and Faber, J. (1987) Neutron and X-ray diffraction study of hydrogarnet $Ca_3Al_2(O_4H_4)_3$. American Mineralogist, 72, 756–765.
Lager, G.A., Armbruster, T., Rotella, F.J., and Rossman, G.R. (1989) OH substitution in garnets: X-ray and neutron diffraction, infrared, and geometric-modeling studies. American Mineralogist, 74, 840–851.
Larson, A.C., and Von Dreele, R.B. (1994) General structure analysis system (GSAS). Los Alamos National Laboratory Report LAUR 86-748.
Lutz, H.D. (1995) Correlation of spectroscopic and structural data. In Structure and Bonding, 82, 85–103.
Nakamoto, K., Margoshes, M., and Rundle, R.E. (1955) Stretching frequencies as a function of distances in hydrogen bonds. Journal of the American Chemical Society, 77, 6480–6488.
Nelmes, R.J., Loveday, J.S., Wilson, R.M., Besson, J.M., Pruzan, P., Klotz, S., and Hull, S. (1993) Neutron diffraction study of the structure of deuterated ice VIII to 10 GPa. Physical Review Letters, 71, 1192–1195.
Novak, A. (1974) Hydrogen bonding in solids: Correlation of spectroscopic and crystallographic data. In Structure and Bonding, 18, 177–216.
Novak, G.A., and Gibbs, G.V. (1971) The crystal chemistry of silicate garnets. American Mineralogist, 56, 791–825.
Olijnyk, H., Paris, E., Geiger, C.A., and Lager, G.A. (1991) Compressional study of katoite [$Ca_3Al_2(O_4H_4)_3$] and grossular garnet. Journal of Geophysical Research, 96, 14313–14318.
O'Neill, B., Bass, J.D., Rossman, G.R., Langer, K., and Geiger, C.A. (1988) Elastic properties of hydrous garnets. Eos, 69, 1407.
Owrutsky, J.C., Rosenbaum, N.H., Tack, L.M., and Saykally, R.J. (1985) The vibration-rotation spectrum of the hydroxide ion (OH^-). Journal of Chemical Physics, 83, 5338–5339.
Parise, J.B., Leinenweber, K., Weidner, D.J., Tan, K., and Von Dreele, R.B. (1994) Pressure-induced H bonding: Neutron diffraction study of brucite, $Mg(OH)_2$, to 9.3 GPa. American Mineralogist, 79, 193–196.
Rietveld, H.M. (1969) A profile refinement method for nuclear and magnetic structures. Journal of Applied Crystallography, 2, 65–71.
Rossman, G.R., and Aines, R.D. (1991) The hydrous component in garnets: Grossular-hydrogrossular. American Mineralogist, 76, 1153–1164.
Smith, R.I., and Hull, S. (1994) User guide for the Polaris Powder Diffractometer at ISIS. Rutherford Appleton Laboratory Report RAL-94-115.
Velde, B., and Martinez, G. (1981) Effect of pressure on OH stretching frequencies in kaolinite and aluminous serpentine. American Mineralogist, 66, 196–200.
Williams, Q. (1992) A vibrational spectroscopic study of hydrogen in high pressure mineral assemblages. In Y. Syono and M.H. Manghnani, Eds., High-pressure research: Application of earth and planetary sciences, Geophysical Monograph 67, American Geophysical Union, 289–296.